C. R. Chimie 21 (2018) 809–813

Contents lists available at ScienceDirect

Comptes Rendus Chimie

www.sciencedirect.com

Preliminary communication/Communication

Facile synthesis of nanoparticles of the molecule-based superconductor κ-(BEDT-TTF)$_2$Cu(NCS)$_2$

Synthèse aisée de nanoparticules du supraconducteur moléculaire κ-(BEDT-TTF)$_2$Cu(NCS)$_2$

Benoît Cormary [a, b], Christophe Faulmann [a, b], Dominique de Caro [a, b, *], Lydie Valade [a, b], Pascale de Caro [c], Belén Ballesteros [d], Jordi Fraxedas [d]

[a] CNRS, LCC (Laboratoire de chimie de coordination), 205, route de Narbonne, BP 44099, 31077 Toulouse cedex 4, France
[b] Université de Toulouse, UPS, INPT, 31077 Toulouse cedex 4, France
[c] Laboratoire de chimie agro-industrielle (LCA), Université de Toulouse, INRA, INPT, Toulouse, France
[d] Catalan Institute of Nanoscience and Nanotechnology (ICN2), CSIC and BIST, Campus UAB, 08193 Bellaterra (Barcelona), Spain

ARTICLE INFO

Article history:
Received 23 April 2018
Accepted 16 July 2018
Available online 17 August 2018

Keywords:
Nanostructures
Donor–acceptor systems
Superconductors
Electron microscopy

ABSTRACT

Well-dispersed roughly spherical nano-objects of the molecule-based superconductor κ-(BEDT-TTF)$_2$Cu(NCS)$_2$ have been prepared in an organic solution by using an easy synthetic route. Long alkyl-chain aconitate esters have been used as growth controlling agents. Nano-objects exhibiting sizes in the 35–120 nm range are made of aggregated individual smaller nanoparticles ranging from 3 to 10 nm. Nanoparticle powders have been studied by X-ray diffraction, high resolution electron microscopy and atomic force microscopy in the conductivity mode.

Mots clé:
Nanostructures
Systèmes donneur–accepteur
Supraconducteurs
Microscopie électronique

RÉSUMÉ

Des nano-objets sphériques et bien dispersés du supraconducteur moléculaire κ-(BEDT-TTF)$_2$Cu(NCS)$_2$ ont été préparés en solution organique à l'aide d'une méthode de synthèse relativement aisée. Des aconitates à longue chaîne alkyle ont été utilisés comme régulateurs de croissance. Ces nano-objets de taille comprise entre 35 et 120 nm sont constitués de petites particules dont le diamètre individuel est de l'ordre de 3 à 10 nm. Les poudres nanoparticulaires ont été étudiées par diffraction des rayons X, par microscopie électronique à haute résolution et enfin par microscopie à force atomique en mode conducteur.

* Corresponding author.
E-mail address: dominique.decaro@lcc-toulouse.fr (D. de Caro).

https://doi.org/10.1016/j.crci.2018.07.006

1. Introduction

The sulfur-based bis(ethylenedithio)tetrathiafulvalene (BEDT-TTF, Fig. 1) molecule has been used as a building block for a large number of organic conductors, some of which are superconductors at ambient pressure [1]. Salts with coordination complex anions such as κ-$(BEDT\text{-}TTF)_2X$, where $X = Cu(NCS)_2$, $Cu[N(CN)_2]Br$, $Cu[N(CN)_2]Cl$ or $Cu(CN)[N(CN)_2]$, exhibit superconductivity with T_C exceeding 10 K [1]. Among them, single crystals of κ-$(BEDT\text{-}TTF)_2Cu(NCS)_2$ show a T_C of 10.4 K. Recently, thin single crystals of κ-$(BEDT\text{-}TTF)_2Cu(NCS)_2$ have been grown on Au patterned Si/SiO_2 wafers [2]. Surface-conductive polymer composites based on $(BEDT\text{-}TTF)_2Cu(NCS)_2$ have also been reported [3]. To our knowledge, the first nanostructuration and organization of this conductor has been described by Y. Li et al. [4]. They have fabricated nanorod arrays of κ-$(BEDT\text{-}TTF)_2Cu(NCS)_2$ supported on platinum foil or indium tin oxide glass. The morphologies of the nanorods have been controlled by adjusting the growth current density. We have recently demonstrated simple chemical or electrochemical ways for preparing nanoparticles of $(BEDT\text{-}TTF)_3Cl_2$, $(BEDT\text{-}TTF)_2Br$ and $(BEDT\text{-}TTF)_2I_3$ using ionic liquids, long-chain ammonium salts or neutral amphiphilic molecules as growth controlling agents [5–7]. Among amphiphilic molecules, polycarboxylates have never been studied as growth controlling agents for the preparation of organic-based nanostructured materials. However, trimethyl aconitate derivatives have already been cited as green surfactants [8]. In the present communication, we report on the preparation of $(BEDT\text{-}TTF)_2Cu(NCS)_2$ nanoparticles using biobased amphiphilic molecules, namely *n*-dodecanoic acid ($n\text{-}C_{11}H_{23}COOH$) and aconitate esters bearing one or several $C_{12}H_{25}$ group(s).

2. Results and discussion

A previous study has shown the efficiency of long hydrocarbon chain imines as growth controlling agents for the selective synthesis of $(BEDT\text{-}TTF)_2I_3$ nanoparticles [7]. In the present work, we have studied the growth of $(BEDT\text{-}TTF)_2Cu(NCS)_2$ as nano-objects by using another class of neutral amphiphilic molecules with an ethylenic group, aconitate esters bearing one or several C_{12} hydrocarbon chains (AE, Fig. 2). *n*-dodecanoic acid (*n*-DA) has also been chosen as a conventional amphiphilic molecule with the same C_{12} hydrocarbon chain.

Hydrophilic-lipophilic balances (HLB) of *n*-DA or AE are calculated according to Griffin's empirical method [9]: 4.2 for *n*-DA, 10.0 for the monoaconitate, 6.4 for the diaconitate, and 5.0 for the triaconitate. Taking into account the composition of esters (see the Experimental section below), a value of 6.0 is found. *n*-DA and AE belong to the category of emulsifiers dedicated to the dispersion of water in oil.

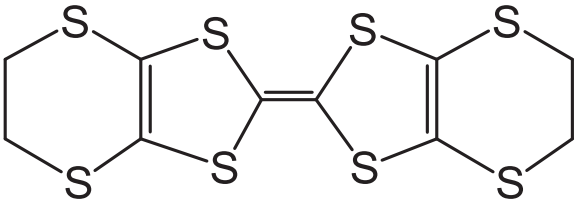

Fig. 1. Molecular structure of BEDT-TTF.

The chemical oxidation of BEDT-TTF using the copper(II) complex $Cu(NCS)_2$ in a tetrahydrofuran solution containing *n*-DA or AE leads to an air stable dark brown powder. Whatever be the amphiphilic moiety used, X-ray diffraction patterns are very similar and confirm unambiguously that the κ-$(BEDT\text{-}TTF)_2Cu(NCS)_2$ phase is obtained (Fig. 3) [10].

Infrared spectra are also in agreement with those for polycrystalline pressed samples of $(BEDT\text{-}TTF)_2Cu(NCS)_2$ (see the Experimental section below) [11]. It should be noted that the absence of C=O vibrational modes implies the absence of *n*-DA or AE within the powders. When the synthesis is conducted in the presence of *n*-DA (3 molar equivalents vs. BEDT-TTF), low-magnification electron micrographs evidence strings of particles as well as few dispersed particles (Fig. 4). When AE is used (3 molar equivalents vs. BEDT-TTF), exclusively well-dispersed roughly spherical nano-objects are observed (sizes in the 35–120 nm range, Fig. 5). Similar electron micrographs are obtained for particles prepared in the presence of 5 and 10 molar equivalents versus BEDT-TTF. As mentioned above (IR spectroscopy), the amphiphilic molecules (*n*-DA or AE) are not present in the nanopowders. However, their HLB values confer them an appropriate behavior to control the growth of $(BEDT\text{-}TTF)_2Cu(NCS)_2$ as nano-objects in the solution. It is noticeable that aconitate esters lead to a better dispersion of the nano-objects, showing that the chemical structure of the emulsifier has also a significant role. Indeed, the presence of an ethylenic group in aconitate esters would favor a better controlled growth via π–π interactions with the multiple bonds of the BEDT-TTF molecule, as previously observed [7]. Moreover, the use of more sterically hindered molecules such as AE (in comparison to *n*-DA) would explain the better state of dispersion observed in the TEM micrographs. The HRTEM images of $(BEDT\text{-}TTF)_2Cu(NCS)_2$ prepared in the presence of AE are shown in Fig. 6. Nano-objects are actually made of aggregated individual smaller nanoparticles ranging from three to about 10 nm, which are also found isolated on the TEM grid. The nanoparticles exhibit a high degree of crystallinity, and spacings of 2.1 Å are measured. As previously observed for $(BEDT\text{-}TTF)_2I_3$ nanoparticles [7], the large interplanar spacings corresponding to the main crystallographic planes in the structure (*e.g.*, 15.2 Å for (100), 12.3 Å for (001) or 8.3 Å for (101)) are not visible, most probably due to radiation damage under the 200 kV electron beam. Indeed, organic specimens are particularly sensitive to radiolysis damage, where the electron-electron interactions break chemical bonds and can contribute to creating new structures [12].

Fig. 7 shows an I–V curve of an individual 40 nm high nanoparticle (NP) aggregate measured with an AFM. The deviation from the linear ohmic behaviour that would be expected from a metallic NP arises from the involved boundaries, *i.e.*, NP-NP, tip-NP and substrate-NP. From the curve, an effective resistance may be obtained from the slope at $V = 0$, but such magnitude is very much dependent on the applied pressure on the NP aggregate, a magnitude

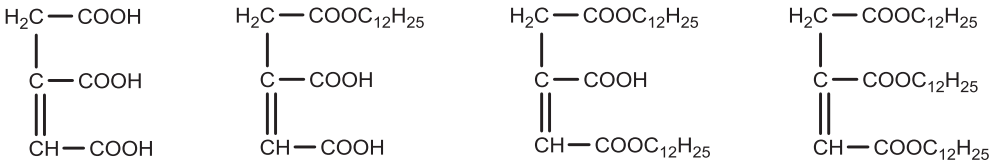

Fig. 2. Molecular structures of aconitic acid and mono-, di- and tridodecyl aconitates. For mono- and didodecyl aconitates, only one in three molecules has been drawn, the other molecules are obtained by permutation of the $C_{12}H_{25}$ substituent(s).

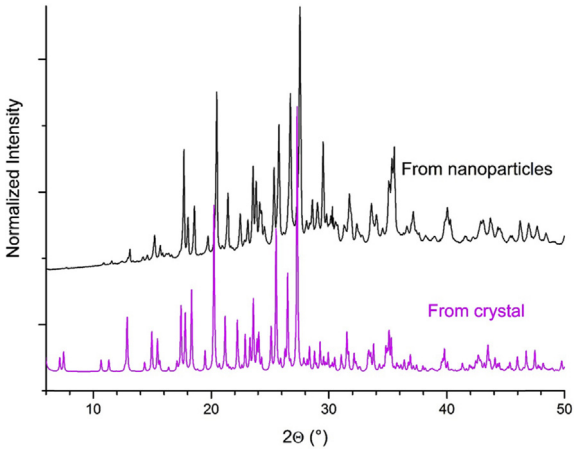

Fig. 3. XRD pattern of $(BEDT\text{-}TTF)_2Cu(NCS)_2$ grown in the presence of *n*-DA (top) and simulated from $(BEDT\text{-}TTF)_2Cu(NCS)_2$ single crystals (bottom).

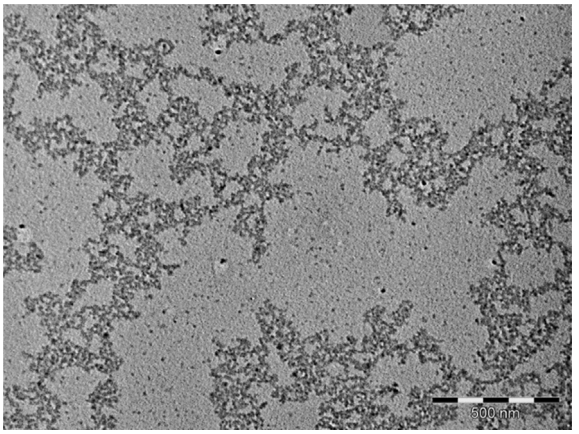

Fig. 4. Low-magnification electron micrograph of $(BEDT\text{-}TTF)_2Cu(NCS)_2$ prepared in the presence of *n*-DA (bar = 500 nm).

that can only be estimated with a large source of error due to the unknown contact area between the tip and the aggregate and that can easily reach the GPa range. Note the asymmetric shape of the curve which suggests a rectifying character of the NP aggregate. Similar curves were obtained for $(BEDT\text{-}TTF)_2I_3$ nanoparticle aggregates [7].

3. Conclusion

We have isolated the first nanoparticles of the molecule-based superconductor κ-$(BEDT\text{-}TTF)_2Cu(NCS)_2$, using

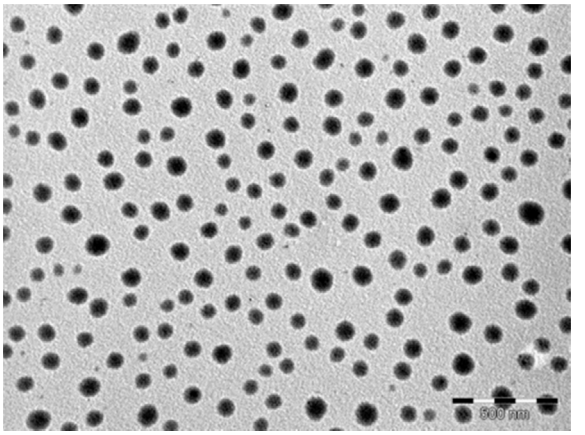

Fig. 5. Low-magnification electron micrograph of $(BEDT\text{-}TTF)_2Cu(NCS)_2$ prepared in the presence of AE (bar = 500 nm).

aconitate esters bearing $C_{12}H_{25}$ alkyl groups as growth controlling agents. Under the conditions explored, roughly spherical aggregates of very small individual nanoparticles have been obtained. We are currently investigating the use of other aconitate esters bearing C_{18} oleyl groups with the aim of preparing well dispersed 2–10 nm particles. We have also planned to investigate the superconducting transition of the nanoparticle powders.

4. Experimental section

4.1. General information

All syntheses are performed under an argon atmosphere. Tetrahydrofuran (THF) is distilled and stored under argon prior to use. BEDT-TTF and *n*-dodecanoic acid are commercially available and used as received. The $Cu(NCS)_2$ complex is prepared following a procedure described in the literature [13].

4.2. Synthesis of aconitate esters

Aconitate esters are prepared as follows: dodecan-1-ol (12.1 g, 65 mmol) is put in a flask while heating at 40 °C, before adding *trans*-aconitic acid (7.5 g, 43 mmol) under stirring. After complete solubilisation of *trans*-aconitic acid in dodecan-1-ol, 0.24 g of concentrated sulfuric acid is added. The resulting mixture is then stirred at 100 °C for 5 h, the water being trapped by the molecular sieve placed above the flask. After cooling down to room temperature, 20 mL of ethyl acetate are added to the medium and the

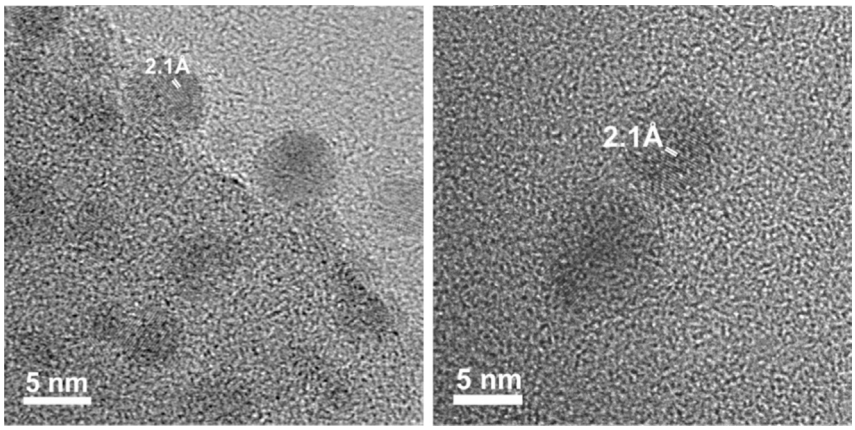

Fig. 6. High-magnification electron micrographs of the $(BEDT\text{-}TTF)_2Cu(NCS)_2$ aggregate (left) and isolated nanoparticles (right) prepared in the presence of AE.

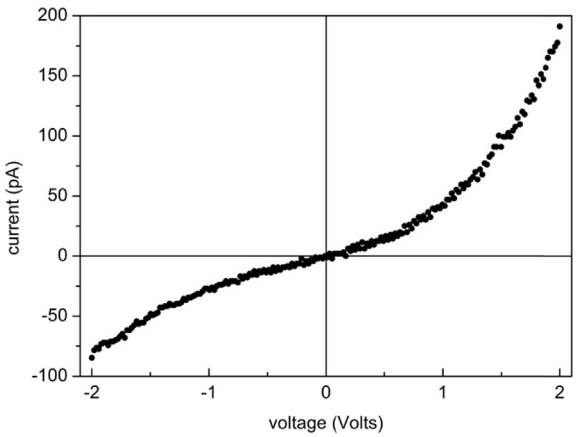

Fig. 7. Current-voltage (I–V) curve of an individual NP aggregate with a height of 40 nm measured with an AFM in the conductivity mode.

organic phase is washed three times with 10 mL of water. Ethyl acetate is then evaporated under vacuum to obtain about 10 g of aconitate esters. The ester composition is calculated from ^1H NMR data, using the integrations of ethylenic protons whose chemical shifts are 7.00, 7.03, and 7.06 ppm (for monododecyl esters), 6.95, 6.97, and 7.01 ppm (for didodecyl esters), and 6.93 ppm (for the tridodecyl ester). The composition is as follows: monododecyl, 17%; didodecyl, 16%; tridodecyl, 67%.

4.3. Synthesis of $(BEDT\text{-}TTF)_2Cu(NCS)_2$ nanoparticles

A THF solution (30 mL) of BEDT-TTF (85 mg, 0.22 mmol), $Cu(NCS)_2$ (20 mg, 0.11 mmol) and *n*-dodecanoic acid (132 mg, 0.66 mmol) [or 400 mg of the mixture of aconitate esters, *i.e.*, 0.66 mmol, based on the average molar mass] is heated under reflux for 1h15. The resulting suspension is then filtered hot. The precipitate is washed with THF (2×20 mL), diethylether (2×20 mL), and finally dried under vacuum for 10 h to obtain a dark brown powder (yield: 70%). IR: 875 (ν_{C-S}), 1162 and 1249 (δ_{C-C-H}), 1313 ($\nu_{C=C}$), 1408 (methylene deformation), 1447 ($\nu_{C=C}$), 2067 and 2110 ($\nu_{N=C}$), 2919 and 2963 (ν_{C-H}) cm^{-1}.

4.4. Equipment and characterization details

Infrared spectra are obtained at room temperature (in KBr matrix) on a Perkin Elmer Spectrum GX spectrophotometer. X-ray diffraction data are collected at room temperature with a Bruker D8 Advance diffractometer working in the Bragg-Brentano configuration (θ-θ) using Ni filtered CuK_α radiation (0.15418 nm) and fitted with a SuperSpeed Vantec Detector. For electron microscopy, the samples are sonicated, dispersed in acetonitrile, and placed onto a holey carbon-copper support grid. Low-magnification TEM experiments are performed on a JEOL Model JEM 1011 operating at 100 kV. HRTEM images are recorded with an FEI Tecnai F20 HRTEM operating at 200 kV. The I–V curves of an individual NP aggregate are acquired on an AFM Smarts SPM 1000 (AIST-NT) in conductivity mode using Pt-coated cantilever tips (HQ:NSC15/Pt fromMicroMash). The NPs are dispersed on a gold substrate.

Acknowledgements

B. Cormary thanks the Centre National de la Recherche Scientifique (CNRS) for a post-doctoral fellowship. The authors thank S. Ladeira for XRD characterization and M. Tassé for AFM and I–V curves. The authors also thank the GDRI HC3A (Heteroelements and Coordination Chemistry: from Concepts to Applications). The ICN2 is funded by the CERCA programme/Generalitat de Catalunya. The ICN2 is supported by the Severo Ochoa programme of the Spanish Ministry of Economy, Industry and Competitiveness (MINECO, grant no. SEV-2013-0295).

References

[1] T. Ishiguro, K. Yamaji, G. Saito, Organic Superconductors, 2nd ed., Springer, Heidelberg, 1998.
[2] A.A. Bardin, P.L. Burn, S.-C. Lo, B.J. Powell, Phys. Status Solidi B 249 (2012) 979–984.
[3] J.K. Jeszka, A. Sroczyńska, A. Tracz, H. Müller, Synth. Met. 94 (1998) 31–34.
[4] C. Huang, Y. Zhang, H. Liu, S. Cui, C. Wang, L. Jiang, D. Yu, Y. Li, D. Zhu, J. Phys. Chem. C 111 (2007) 3544–3547.
[5] D. de Caro, L. Valade, C. Faulmann, K. Jacob, D. Van Dorsselaer, I. Chtioui, L. Salmon, A. Sabbar, S. El Hajjaji, E. Pérez, S. Franceschi, J. Fraxedas, New J. Chem. 37 (2013) 3331–3336.

[6] D. de Caro, C. Faulmann, L. Valade, K. Jacob, I. Chtioui, S. Foulal, P. de Caro, M. Bergez-Lacoste, J. Fraxedas, B. Ballesteros, J.S. Brooks, E. Steven, L.E. Winter, Eur. J. Inorg. Chem. (2014) 4010–4016.
[7] I. Chtioui-Gay, C. Faulmann, D. de Caro, K. Jacob, L. Valade, P. de Caro, J. Fraxedas, B. Ballesteros, E. Steven, E.S. Choi, M. Lee, S.M. Benjamin, E. Yvenou, J.-P. Simonato, A. Carella, J. Mater. Chem. C 4 (2016) 7449–7454.
[8] Y. Okada, T. Banno, K. Toshima, S. Matsumura, J. Oleo Sci. 58 (2009) 519–528.
[9] A.W. Adamson, A.P. Gast, Physical Chemistry of Surfaces, 6th ed., John Wiley & Sons, New-York, 1997.
[10] K.D. Carlson, U. Geiser, A.M. Kini, H.H. Wang, L.K. Montgomery, W.K. Kwok, M.A. Beno, J.M. Williams, C.S. Cariss, Inorg. Chem. 27 (1988) 965–967.
[11] R. Zamboni, D. Schweitzer, H.J. Keller, C. Taliani, Z. Naturforsch. 44a (1989) 295–299.
[12] R.F. Egerton, P. Li, M. Malac, Micron 35 (2004) 399–409.
[13] H. Müller, Y. Ueba, Bull. Chem. Soc. Jpn. 66 (1993) 32–39.